Stator and Rotor Shape Designs of Interior Permanent Magnet Type Brushless DC Motor for Reducing Torque Fluctuation

Sun-Kwon Lee[1,2], Gyu-Hong Kang[1], Jin Hur[2], and Byoung-Woo Kim[2]

[1]Korea Marine Equipment Research Institute, SongJeong-dong, GangSeo-gu, Busan, 1631-10, Korea
[2]Department of Electrical Engineering, University of Ulsan, 102. Street Dae-hak, Nam-gu, Ulsan 680-749, Korea

This paper presents the stator and rotor shape designs in interior permanent magnet (IPM) type brushless dc (BLDC) motor for reducing torque fluctuation. The partly enlarged air-gap made by rotor unequal out diameter and stator core structure with pole shoe modification is introduced. The torque ripple reduction is achieved by upgrading torque value at minimum torque position and their detail characteristics are compared. The final stator and rotor shape of IPM type BLDC motor is decided by design of experiments (DOE) process. The magnetic field and torque characteristics are analyzed by 2 dimensional (2D) finite element analysis (FEA) and their performances are validated by experimental results.

***Index Terms*—Cogging torque, finite element analysis, IPM type BLDC, torque ripple reduction.**

I. Introduction

In comparison to surface-mounted PM (SPM) motors, IPM motors are more attractive option for various applications because of their high torque density, wide speed range, excellent efficiency and robustness [1]. However, the electromagnetic excitation caused by variations in the torque fluctuation as a result of the magnetization distribution of the PM according to rotor position generates vibration and noise, which is a major problem [2], [3]. The removal of torque fluctuation is always very crucial for most applications which require smooth running [4].

Torque ripple caused by rotor field and stator current, is affected by harmonic components of radial flux density. The cogging torque is generated from the interaction between the air-gap flux distribution and stator slotting structure. The torque fluctuation reduction can be achieved by minimizing torque ripple and cogging torque [5].

Thus, many previous researchers [2]–[9] dealt with torque fluctuation reduction problems of PM motors. Hur and colleagues [2] proposed 3rd harmonic elimination method to reduce cogging torque. Kang [4] introduced the analytical approach to calculate the cogging torque of IPM motor. The rotor flux barrier optimization with response surface method (RSM) of double-barrier type IPMSM also studied by Fang and colleagues [5]. The rotor flux barrier design of PM-assisted synchronous reluctance motor for torque ripple reduction is also studied [6]. The holes arrangement in the rotor had been studied for distributed winding IPM motor [7]. The cutting of rotor out diameter technique for distributed winding type IPM motor [8] and multiobjective optimization technique by Taguchi method [9] are introduced.

This paper studied the shape design of stator and rotor core structure of concentrated winding IPM type BLDC motor to reduce cogging torque and torque ripple. The partly enlarged air-gap made by modifying the stator core and rotor core structure is introduced. The flux distribution in the magnetic circuit was investigated to compare the relationship between torque ripple and flux density of air-gap in detail. The final core structure is decided by DOE to select the optimal points of several design factors.

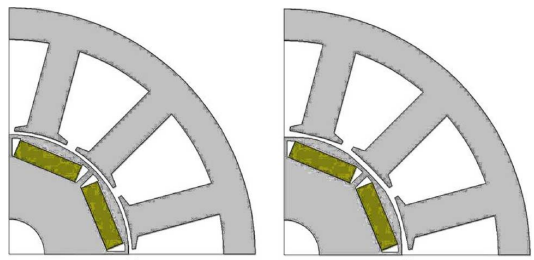

Fig. 1. Quadrant structures of initial and improved models. (a) Initial model. (b) Improved model without holes ("Nohole").

II. Initial and Improved Models

Fig. 1 shows the cross sections of initial and improved design which is obtained by DOE for 8 pole-12 slot IPM type BLDC motor respectively. The stator has three phase concentrated windings and rotor is single layer IPM structure. The main dimensions and specifications are listed in Table I. The stator out diameter is 140 mm and the high power density rare-earth magnets of which residual induction is 1.21(T) are used. The improved model has partly enlarged air-gap length by unequal rotor out diameter and stator core cutting.

III. Torque Fluctuation Reduction

A. Torque Fluctuation Reduction by DOE

The IPM motor design is very complicated owing to many design factors, as well as the mechanical robustness between each part must be fully considered [5]. Therefore, the DOE such as response surface methodology (RSM) by using Minitab 14 is adopted to optimize multi parameters efficiently. The unequal rotor out diameter and stator cutting dimensions are confirmed. Fig. 2 shows the design parameters and Fig. 3 presents the final parameters from DOE results. The Px and Py in Fig. 2 are the

Manuscript received March 02, 2012; revised May 03, 2012 and May 16, 2012; accepted May 18, 2012. Date of current version October 19, 2012. Corresponding author: J. Hur (e-mail: jinhur@ulsan.ac.kr).

Color versions of one or more of the figures in this paper are available online at http://ieeexplore.ieee.org.

Digital Object Identifier 10.1109/TMAG.2012.2201455

TABLE I
MAIN DIMENSIONS AND SPECIFICATIONS

Items	Values	Unit
Stator out diameter	140	mm
Rotor out diameter	68	
Air gap length	1.0	mm
Stack length	43	mm
Residual induction	1.21	Tesla
Rated rpm	3,600	mm
Rated current	55	Amax
Pole/slot	8/12	

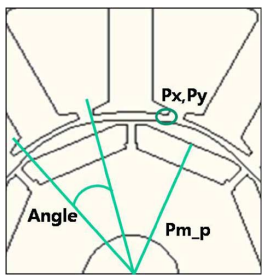

Fig. 2. Design parameters for DOE.

x and y edge points of stator pole shoe respectively. The minimum inner diameter of stator is fixed, so the Px and Py make uneven stator inner diameter shape and different slot open size. The Pm_p is the distance between center point to permanent magnet which those variation makes unequal air gap length due to change of rotor outside cutting size. The Angle stands for the angle of maximum rotor out diameter. The design objectives and parameters are given as

- Design objectives:

$$Y_{cog} \leq 6(\%), Y_{Tavg} \geq 5.0\ (\mathrm{Nm}), Y_{Tripple} \leq 25(\%)$$

- Design parameters:

$$X_{Angle} : 6 \sim 13(^{\circ}), X_{Pm\_p} : 26.1 \sim 26.4\ (\mathrm{mm}),$$
$$X_{Px} : 34.2 \sim 34.7\ (\mathrm{mm}), X_{Py} : 7.3 \sim 8.5\ (\mathrm{mm}).$$

X_{Angle} represents design parameter of angle as in Fig. 2 and Y_{cog} means the results of cogging torque rates to average torque. Tavg stands for average torque and Tripple means percentage of ripple torque value to average torque.

It is found that the desired minimum points of torque ripple and cogging torque cannot be achieved at the same point. Therefore, the optimum point is selected as possible as close to satisfy all requirements. The partly enlarged air gap shape made by rotor out diameter gives main contribution for reducing cogging torque and torque ripple. The shape modification of stator pole shoe gives additional improvement as in Fig. 3.

Fig. 4 and Fig. 5 show that the cogging torque and torque ripple analysis results for each model. Results show that the cogging torque and torque ripple of improved model was reduced compare to initial model. The ratio to average torque of cogging torque is achieved 5.6% from 19.5% and the peak to peak value of torque ripple ratio to average torque is 21% from

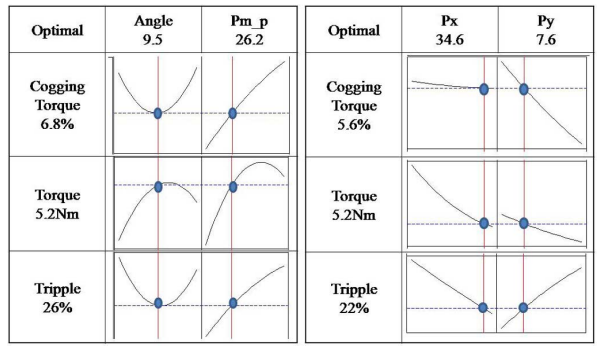

Fig. 3. Response of design objectives from DOE results.

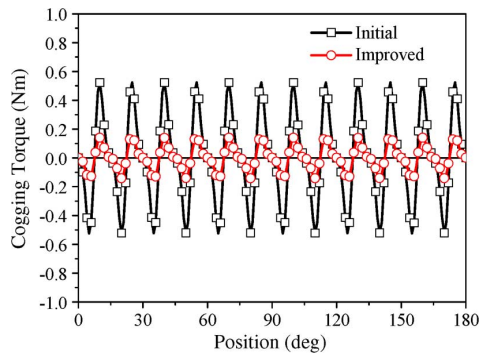

Fig. 4. Cogging torque comparison between initial and improved models.

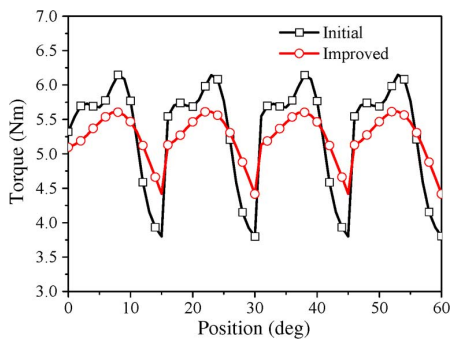

Fig. 5. Commutating torque comparison between initial and improved models.

44.1%. Fig. 6 presents the phase back EMF waveform and their harmonics of initial and improved model at 1,492 rpm. The level of EMF value is almost same but their waveform is lightly different due to partly enlarged air-gap structure. The improved model has less harmonic distortion compare to initial model as in Fig. 6(b). This back EMF harmonic comparison result gives indirect validation of reduction of torque fluctuation with experimental results which is described at further section.

B. Discussions About Torque Ripple

The commutating torque ripple can be reduced by upgrading torque value at minimum points and downsizing at maximum torque points respectively as in Fig. 7. Position #1 and #2 mean the maximum torque point and minimum torque point respectively. To solve the problem, the flux passing through the rotor pole should be reduced at minimum torque position. The combinations of partly enlarged air-gap, holes in rotor make that

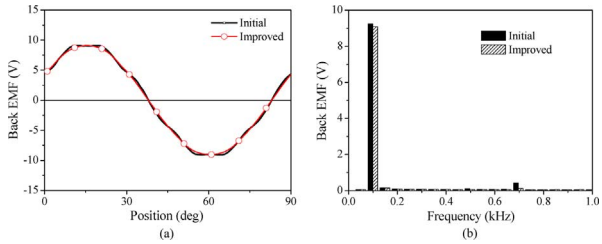

Fig. 6. Phase back EMF comparison between initial and improved models. (a) Back EMF. (b) Harmonic components.

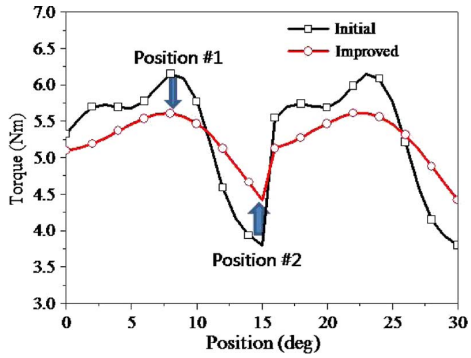

Fig. 7. Commutating torque behavior according to rotor position.

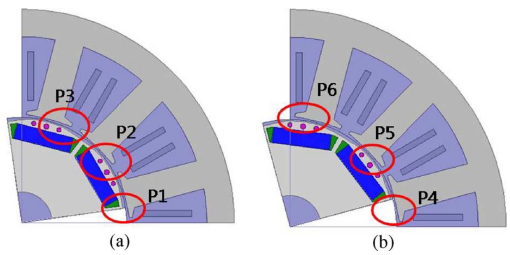

Fig. 8. Maximum and minimum torque position. (a) Maximum torque positions. (b) Minimum torque position.

possible. The air-gap torque distribution can be calculated by Maxwell stress tensor as

$$P_t = \frac{B_n B_t}{\mu_0} \tag{1}$$

where, P_t: tangential components of force density; B_n: normal components of magnetic flux density on contour; B_t: tangential components of magnetic flux density on contour; μ_0: magnetic permeability of air.

The torque at each point can be computed by line integral of tensor on the contour. Fig. 8 shows the relationship between rotor position with response to maximum and minimum torque generating position. Fig. 9 illustrates the comparison results of air-gap torque distribution calculated from (1) at maximum and minimum torque generating position. "Nohole" model has same rotor structure with improved model whether holes in rotor or not. The computational contour is located at the middle of the air-gap. P1, P2, P3, P4, P5 and P6 are the same positions displayed in Fig. 8. The torque value of improved model at Position #1 which is maximum torque position as in Fig. 7 has less

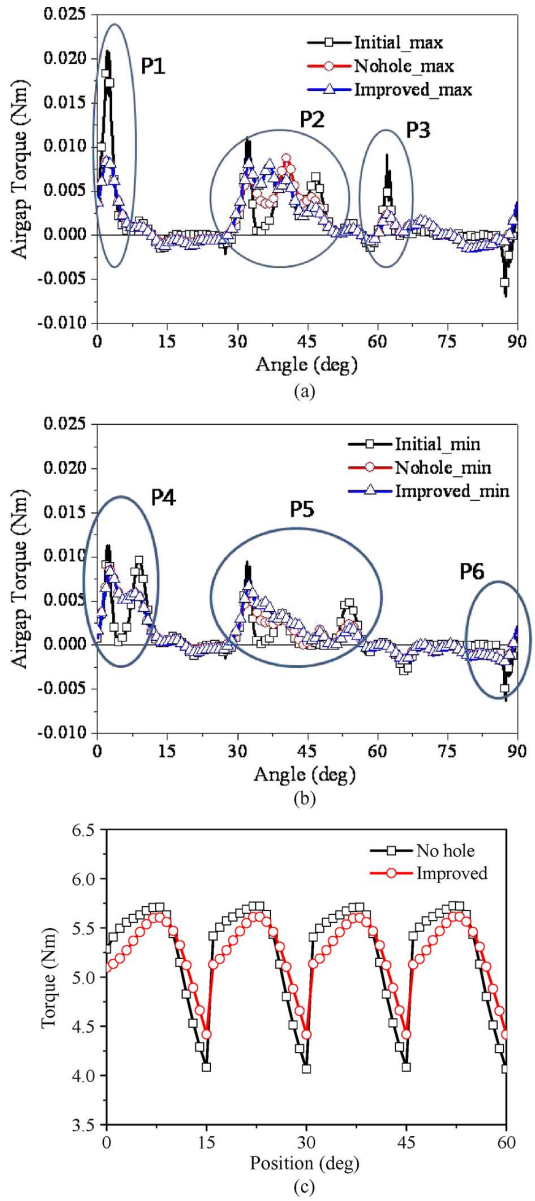

Fig. 9. Air-gap torque distribution analysis. (a) Maximum torque positions. (b) Minimum torque position. (c) Torque comparison with and without holes.

than that of initial model whereas torque is upgraded at Position #2. Therefore the peak to peak value of output torque can be reduced significantly. The peak to peak torque reduced from 2.5 (Nm) to 1.1 (Nm), so ripple reduction ratio exceed 56%. The air-gap torque distribution in Fig. 9(a) says that P1 and P3 torque of initial model make increase the total torque at Position #1 whereas improved model torque at P4, P5 and P6 increase. Center holes in rotor play a role to increase the torque value at P5 by slightly enlargement of tangential component of flux density through distortion of flux path as in the Fig. 10. The combinations of partly enlarged air-gap, flux barrier and side holes increase torque at P5 and P6, whereas initial model generates reverse torque. Therefore, the torque ripple reduces with increase of the resultant torque summed along air-gap contour at minimum torque generating position. The ripple torque reduction effects of holes arrangement in rotor core is shown in Fig. 9(c).

(a) (b)

Fig. 10. Flux lines of improved model. (a) Maximum torque positions. (b) Minimum torque position.

(a) (b)

Fig. 11. Prototype structure and test set up. (a) Structure of prototype. (b) Test set up.

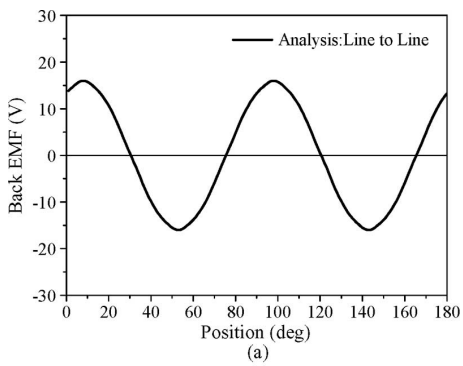

(a) (b)

Fig. 12. No load back EMF measurement. (a) Analysis. (b) Measurement.

IV. Experiments

Fig. 11 presents the core structure of improved "Nohole" IPM type BLDC motor. The 8 pole-12 slot single layer IPM configuration and concentrated winding were adopted. In order to verify the validity of the design results, the experimental results of back EMF, speed-torque and speed-output are compared. The comparison results of back EMF, speed-torque and speed-output characteristics are shown in Fig. 12 and Fig. 13, respectively. The design and analysis of back EMF characteristic of improved model have good agreement with experimental data as in Fig. 12.

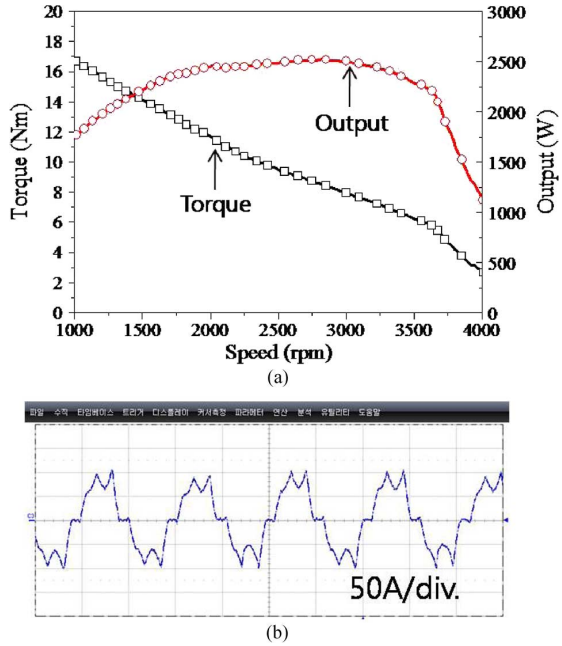

(a) (b)

Fig. 13. Performance test results. (a) Speed-Torque and output power. (b) Current waveform at 3,600 rpm.

Fig. 13 shows the performance test results of prototype motor with phase current waveform. The distortion of test data near 4,000 rpm is occurred from the control characteristics of our test equipments. The torque characteristic according to current agrees with design and analysis results.

V. Conclusion

This paper presents the torque fluctuation reduction method. The partly enlarged air gap length made by unequal rotor out diameter and stator core cutting is introduced. The flux barrier in rotor core is also redesigned. Design of experiments (DOE) method is used to find the optimal points of each design parameter. The comparisons of analysis results show that method is very reliable. The cogging torque is extremely low but the torque ripple reduction rates are not very big in case of square wave operation. Adding holes in rotor core is good solution to overcome this problem, so the additional torque fluctuation reduction can be achieved.

References

[1] T. J. E. Miller, *Design of Brushless Permanent Magnet Motor*. Oxford, U.K.: Clarendon Press, 1994.
[2] J. Hur, J.-W. Reu, B.-W. Kim, and G.-H. Kang, *IEEE Trans. Ind. Appl.*, vol. 47, no. 3, pp. 1300–1309, May/Jun. 2011.
[3] Z. Q. Zhu, D. Ishak, D. Howe, and J. Chen, *IEEE Trans. Industry Applications*, vol. 43, no. 6, pp. 1544–1553, Nov./Dec. 2007.
[4] G.-H. Kang, J.-P. Hong, and G.-T. Kim, *KIEE Int. Trans. Electr. Mach. Energy Conver. Syst.*, vol. 11B, no. 2, pp. 1–8, 2006.
[5] L. Fang, S.-I. Kim, S.-O. Kwon, and J.-P. Hong, *IEEE Trans. Magn.*, vol. 46, no. 6, pp. 2183–2186, Jun. 2010.
[6] N. Bianchi, S. Bolognani, D. Bon, and M. D. Pre, *IEEE Trans. Ind. Appl.*, vol. 45, no. 3, pp. 921–928, May/Jun. 2009.
[7] A. Kioumarsi, M. Moallem, and B. Fahimi, *IEEE Trans. Magn.*, vol. 42, no. 11, pp. 3706–3711, Nov. 2006.
[8] U.-J. Seo, Y.-D. Chun, J.-H. Choi, P.-W. Han, D.-H. Koo, and J. Lee, *IEEE Trans. Magn.*, vol. 47, no. 10, pp. 3240–3243, Oct. 2011.
[9] K.-C. Kim, J. Lee, H.-J. Kim, and D.-H. Koo, *IEEE Trans. Magn.*, vol. 45, no. 3, pp. 1780–1783, Mar. 2009.